

# A Comparative Study of Core Neutronic Computations using DeCART2D/MASTER and Serpent2 for i-SMR Core with GdN-CBA Rods

Seungnam Lee, Woo Jin Lee, Ser Gi Hong\*

Department of Nuclear Engineering, Hanyang University, 222 Wangsimni-ro, Seongdong-gu, Seoul, 04763

\*Corresponding author: hongsergi@hanyang.ac.kr

\***Keywords:** i-SMR Core, GdN-CBA, DeCART2D/MASTER, Serpent2

## 1. Introduction

Small Modular Reactors (SMRs) will play an essential role in achieving carbon-zero energy. In Korea, light water-based SMRs continue to be developed [1]. Most recently, the innovative Small Modular Reactor (i-SMR) has been continuously developed, with enhanced safety, economy, and flexibility.

The i-SMR aims for long-cycle and soluble boron-free (SBF) operation. To simultaneously achieve these goals, an innovative Burnable Absorber (BA) is required for more controllable excess reactivity. The recently developed BAs include CSBA [2], CIMBA [3], enriched Gd<sub>2</sub>O<sub>3</sub> [4], and HIGA [5]. In this study, GdN-CBA [6] was applied to the i-SMR core as the burnable absorber.

In reactor physics calculations, two different methods are used: deterministic and Monte Carlo methods. The deterministic method offers shorter calculation times but requires the resonance approximations and approximations in geometrical modeling while the Monte Carlo method, provides high accuracy with only statistical uncertainties resulted from accurate treatment of energy and spatial description of neutrons but requires high computational cost. Therefore, the Monte Carlo codes are usually used to validate the deterministic codes.

The goal of this study is to conduct the validity of the DeCART2D/MASTER calculations for the i-SMR core using GdN-CBA rods through the comparison with the Serpent2 calculations. In particular, the effect of the control rod depletion, which is an important issue in SBF operation core was analyzed.

## 2. Core Design and Computational Methods

The core specifications were based on the i-SMR design [1]. The specifications of the fuel assemblies (FAs) and the core design with Gadolinium Nitride Coating Burnable Absorber (GdN-CBA) applied were referenced from the previous work [7]. The comparative calculations were conducted both for fuel assembly and core levels.

For two-step deterministic calculations, DeCART2D [8], a lattice code, was used to generate group constants for MASTER [9], a nodal code. Both codes were developed by the Korea Atomic Energy Research Institute (KAERI). For Monte Carlo simulations, Serpent2, developed by VTT Technical Research Centre of Finland, was employed [10].

The ENDF/B-VII.1 cross-section library is used for both DeCART2D (neutron 47 group and gamma 18 group) and Serpent2 (point-wise continuous energy library) codes.

### 2.1 Fuel Assembly and Core Design

As shown in Figure 1, For a GdN-CBA rod, GdN is directly coated onto the UO<sub>2</sub> pellet. The total thickness of the pellet including GdN coating remains constant; therefore, when GdN is applied, the total amount of UO<sub>2</sub> is reduced. In this work, the fuel assembly (FA) uses GdN-CBA rods up to three different thicknesses of GdN coating [11]: 140, 350, and 600 μm. Each rod type and their mesh divisions are depicted in Figure 2, and the parameters of each rod type are summarized in Table I.

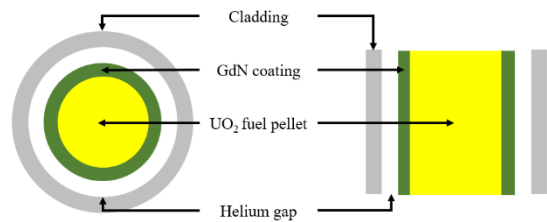


Fig. 1. Radial and axial configurations of GdN-CBA

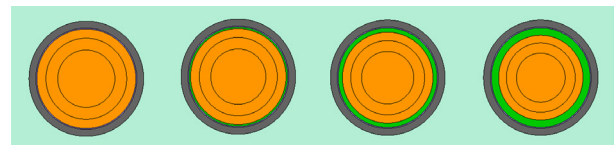


Fig. 2. Configurations and mesh divisions of the fuel rods and Gd-CBA rods (left to right: Normal fuel / a / b / c)

Table I. Design parameters of the GdN-CBA rods

Parameters (cm)	Type a	Type b	Type c
Pellet + GdN coating radius	0.4096	0.4096	0.4096
UO <sub>2</sub> radius	0.3956	0.3746	0.3496
GdN thickness	0.0140	0.0350	0.0600

Table II summarizes the common design parameters of the considered FAs. Table III gives the specific parameters for each FA type used in the core design. The fuel enrichment is uniform across all rods within each FA.

For example, Figure 3 illustrates the B1 FA, which incorporates all rod types.

Table II. Common design parameters of the FAs

Parameters	Unit	Value
Thermal power	MWt	520
FA array		17×17
Number of fuel rods	EA	264
Number of guide tubes	EA	24
UO <sub>2</sub> density	g/cc	10.220
GdN density	g/cc	8.645
Pellet radius	cm	0.4096
Cladding inner radius	cm	0.4178
Cladding outer radius	cm	0.4750
Guide tube inner radius	cm	0.56134
Guide tube outer radius	cm	0.61214
Rod pitch	cm	1.26
Cladding material		Zircaloy-4

Table III. Specific design parameters of each FAs

Parameters	S1	B1	B2	B5	AB	BB
Fuel enrichment (wt%)	3.2	4.0	2.8	4.0	3.2	4.0
Type/	a/4	a/8	a/8	a/8	a/8	a/8
Number of each Rods	b/8	b/8	b/4	b/12	b/12	b/8
	c/8	c/8	c/0	c/0	c/0	c/0

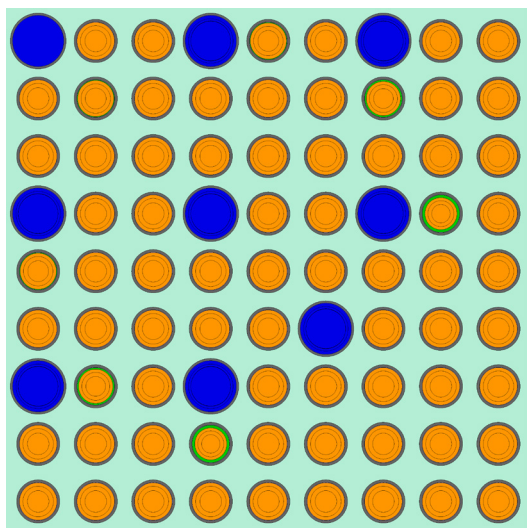


Fig. 3. Configuration of FA type B1 (1/4)

The whole core is depicted in Figure 4. The core is comprised of 69 FAs, each with axial cutbacks. Table IV presents the parameters of the core. All the FAs have a bottom cutback of the same height (i.e., 15 cm). Types S1 and B2 have a top cutback of 25 cm, compared to the 30 cm top cutback of types B1 and B5. All the FAs have an axial reflector of SS-304, and the core is surrounded by radial reflectors, both made of SS-304.

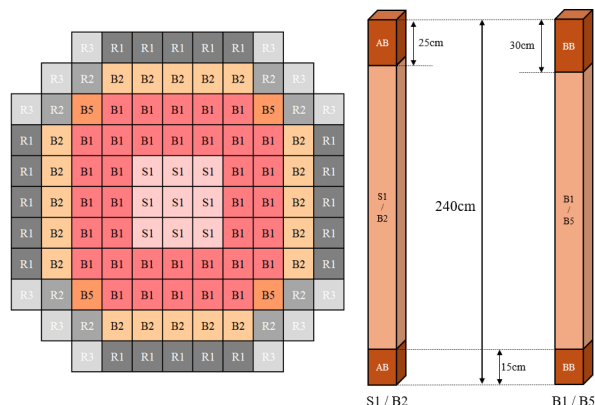


Fig. 4. Radial and axial configurations of the core

Table IV. Design parameters of the core

Parameters	Value
Active core height (cm)	240
Assembly pitch (cm)	21.5
Number of FAs in core S1/B1/B2/B5	9/36/20/4
Reflector material	SS-304

## 2.2 Calculation Conditions

In the FA calculations, the UO<sub>2</sub> pellet was subdivided into 3 rings, while the GdN coating region was subdivided into 8 rings. The fine subdivisions of GdN were implemented to consider for the self-shielding effect in GdN. In the DeCART2D calculations, eight azimuthal and four polar directions for each octant, and 0.01cm ray spacing were used in the MOC calculation. The subgroup option was used for resonance self-shielding treatment.

The MASTER depletion calculations were conducted over 785 EFPDs using the following depletion steps: 0, 10 EFPDs, 50 EFPDs, 100 EFPDs, and the remaining period is divided with 50 EFPDs step size.

Serpent 2 which was developed as a simplified 2D lattice Monte Carlo code has been evolved into a versatile physics tool capable of performing neutron transport and depletion calculations with 3D full-core analysis capabilities. To achieve a standard deviation of less than 10 pcm in  $k_{inf}$  during depletion, 100 inactive cycles and 260 active cycles with 200,000 histories per cycle were adopted.

In full-core calculations, the depletion zones consist of radially independent pins (i.e., no subdivision inside the pellets) and 50 equal-sized axial divisions. To achieve a standard deviation of less than 10 pcm in  $k_{eff}$  during depletion, 200 inactive cycles and 400 active cycles with 400,000 histories per cycle were adopted. The serpent 2 depletion calculations used the same depletion steps as those of DeCART2D and MASTER calculations.

### 3. Results

#### 3.1 Fuel Assembly Calculations

Figure 5 shows the  $k_{inf}$  curves for each FA type using DeCART2D and Serpent. Both codes produce the similar trends of  $k_{inf}$  change curves. The discrepancies in reactivity between the codes were calculated using Eq.(1). While the maximum discrepancies for B1 and BB type FAs were relatively small as 369 pcm and 327 pcm respectively, the B2 FA exhibited the largest discrepancy of 498 pcm at 50 MWd/kg. Therefore, the maximum discrepancy is expected to be less than 500 pcm.

$$error(pcm) = \frac{k_{deterministic} - k_{montecarlo}}{k_{deterministic} * k_{montecarlo}} * 10^5 . (1)$$

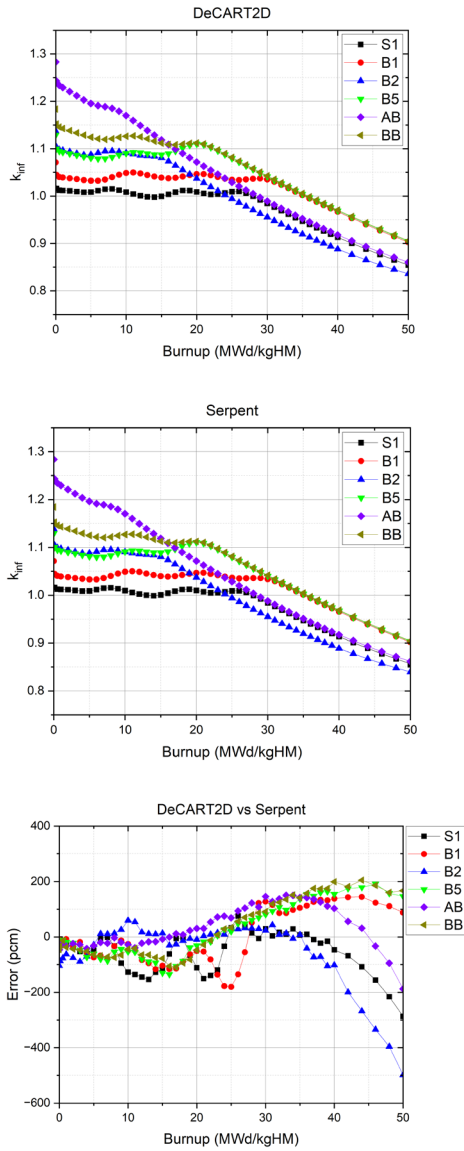


Fig. 5. Evolutions of  $k_{inf}$  for each FA type (Up to down: DeCART2D / Serpent / Error)

Table V. Maximum differences (pcm) of reactivity for each FA type

S1	B1	B2	B5	AB	BB
287	180	498	191	188	205

Table V summarizes the maximum differences in reactivity for each FA type. The B2 type shows the largest discrepancy, followed by S1. B1, B5, AB, and BB types have relatively smaller differences (~200 pcm) between DeCART2D and Serpent results.

#### 3.2 Full-core Calculation

Figure 6 shows the  $k_{eff}$  evolution for both codes. The cycle length was determined using MASTER's critical calculations under ARO (All Rods Out), resulting in 785 EFPDs (Effective Full Power Days) and a burnup at EOC (End of Cycle) of 19.9 MWd/kg. The differences in reactivity between the codes are less than 500 pcm, with the largest value being 448 pcm.

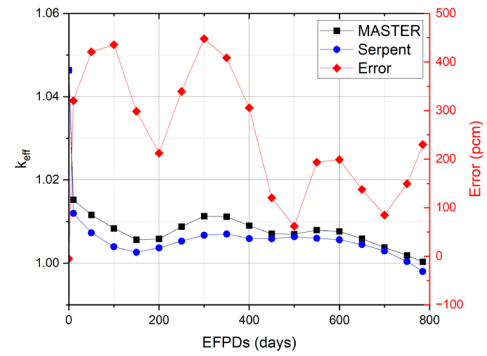


Fig. 6. Comparison of the  $k_{eff}$  evolutions for 3D calculation

MASTER has a control rod search module. It can insert control rod banks and determine their locations to achieve a critical  $k_{eff}$  value. Figure 7 illustrates the locations of the control rod banks used in this core. Figure 8 shows the difference in  $k_{eff}$  values between MASTER and Serpent, with the positions of control rod banks determined by MASTER. When control rods are inserted, the maximum error is 350 pcm.

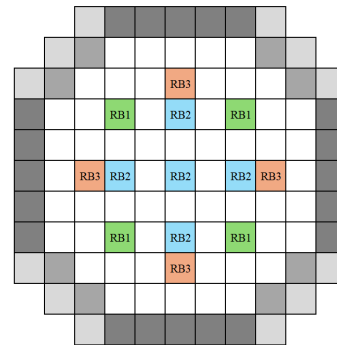


Fig. 7. Configuration of control banks

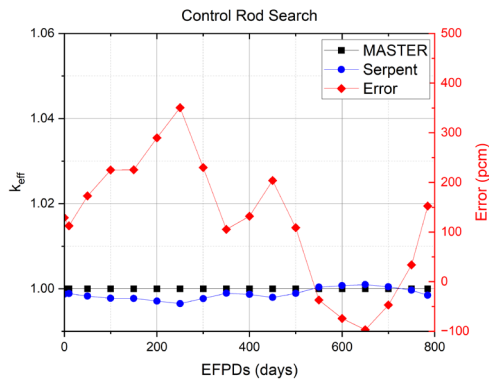


Fig. 8. Comparison of the  $k_{\text{eff}}$  evolutions with the critical control rod positions

### 3.3 CR Depletion Effect

The boron-free reactor maintains criticality through the insertion of control rods. Therefore, the accurate calculation of control rod worth is critical. In the DeCART2D/MASTER system, it is not possible to account for changes in control rod worth due to depletion of the AIC control rod material. However, Serpent2 can designate all materials as burnable, allowing these materials to undergo depletion.

To clearly observe the changes in  $k_{\text{eff}}$  due to depletion of the CR material, all control rods were fully inserted. Figure 9 shows the difference in  $k_{\text{eff}}$  when control rods are inserted, comparing two cases: 1) Serpent2 without AIC as a burnable material, and 2) Serpent2 with AIC as a burnable material. From the results, it was shown that the consideration of the control rod depletion gives  $\sim 300$  pcm difference at EOC.

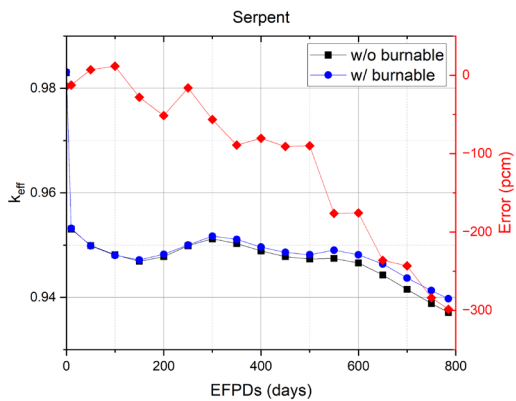


Fig. 9. Comparison of the  $k_{\text{eff}}$  evolutions for CR fully inserted

## 4. Conclusions

For the GdN-CBA based i-SMR, we compared the calculations of the DeCART2D/MASTER and Serpent2.

In fuel assembly calculations, the fuel assemblies having lower uranium enrichments showed higher discrepancies in  $k_{\text{inf}}$  between these two codes and the

maximum discrepancies were about 500 pcm within the maximum discharge burnup of the fuel assemblies in the core. In 3D full-core calculations under ARO, the difference in  $k_{\text{eff}}$  was about 500 pcm during the first cycle. On the other hand, the differences remained within 400 pcm with the critical control rod positions determined by MASTER. The consideration of the control rod depletion gave  $\sim 350$  pcm differences in the Serpent2 calculation from the results obtained without control rod depletion for ARI condition.

## Acknowledgment

This work is financially supported by the Korea Institute of Energy Technology Evaluation and Planning (KETEP) grant funded by the Ministry of Trade, Industry and Energy (MOTIE) of Republic of Korea (No. RS-2024-00398867) and by the Nuclear Safety Research Program through the Regulatory Research Management Agency for SMRS (RMAS) and the Nuclear Safety and Security Commission (NSSC) of the Republic of Korea (No. RS-2024-00509678).

## REFERENCES

- [1] H.O. Kang, B.J. Lee, S.G. Lim, Light water SMR development status in Korea, Nuclear Engineering and Design 419 (2024) 112966. <https://doi.org/10.1016/j.nucengdes.2024.112966>.
- [2] X.H. Nguyen, C. Kim, Y. Kim, An advanced core design for a soluble-boron-free small modular reactor ATOM with centrally-shielded burnable absorber, Nuclear Engineering and Technology 51 (2019) 369–376. <https://doi.org/10.1016/j.net.2018.10.016>.
- [3] Y. Jo, H.C. Shin, Design optimization of cylindrical burnable absorber inserted into annular fuel pellets for soluble-boron-free SMR, Nuclear Engineering and Technology 54 (2022) 1464–1470. <https://doi.org/10.1016/j.net.2021.09.043>.
- [4] J.S. Kim, B.H. Cho, S.G. Hong, Applicability Evaluation of Enriched Gadolinium as a Burnable Absorber in Assembly Level for Boron-Free i-SMR core, Transactions of the Korean Nuclear Society Spring Meeting, Jeju, Korea, May 19-20, 2022.
- [5] J.S. Kim, T.S. Jung, J. Yoon, Reactor core design with practical gadolinia burnable absorbers for soluble boron-free operation in the innovative SMR, Nuclear Engineering and Technology 56 (2024) 3144–3154. <https://doi.org/10.1016/j.net.2024.03.015>.
- [6] S.H. Cho, S.G. Hong, A Novel Burnable Absorber for Small Modular Reactors: Gadolinium (III) Nitride Coating, Transaction of the Korean Nuclear Society Spring Meeting, Jeju, Korea, May 18-19, 2023.
- [7] W.J. Lee, S.H. Cho, S.G. Hong, Performance Analysis of Long-Cycle Small PWR Core with Coating Type Burnable Absorber and Different Reflectors, Proceedings of the Reactor Physics Asia 2023 (RPHA2023) Conference, Gyeongju, Korea, October 24-26, 2023.
- [8] J.Y. Cho, et al., DeCART2D v1.0 User's Manual, KAERI/TR-5116/2013, Korea Atomic Energy Research Institute, 2013.

- [9] J.Y. Cho, et al., MASTER v4.0 User's Manual, KAERI/UM-41/2016, Korea Atomic Energy Research Institute, 2016.
- [10] J. Leppänen, M. Pusa, T. Viitanen, V. Valtavirta, T. Kaltiaisenaho, The Serpent Monte Carlo code: Status, development and applications in 2013, *Annals of Nuclear Energy* 82 (2015) 142–150.  
<https://doi.org/10.1016/j.anucene.2014.08.024>.
- [11] W.J. Lee, S.H. Cho, S.G. Hong, Neutronic Simulation of Daily Load Following Operation in a PWR-based SMR core, to be published in the Transactions of the American Nuclear Society Winter Meeting, Orlando, FL, November 17-21, 2024.